

A crystalline orbital study of polydiacetylenes

Motoi Tobita, So Hirata, and Rodney J. Bartlett^{a)}

Quantum Theory Project, University of Florida, Gainesville, Florida 32611

(Received 14 December 2000; accepted 8 March 2001)

The electronic and structural properties of the ground and excited states of infinite polydiacetylene chains in acetylenic (PDA) and butatrienic (PBT) structures are studied by a series of *ab initio* crystalline orbital and linear-combination-of-atomic-orbital periodic density functional theory methods. A complete geometry optimization is performed for PDA and PBT with analytical energy gradient techniques at the Hartree–Fock (HF) and Becke3–Lee–Yang–Parr (B3LYP) levels. The HF/6-31G* and B3LYP/6-31G* reproduce the experimental geometrical parameters of substituted polydiacetylenes with a PDA-like structure. We compute the relative stability and the potential energy curves along the structural transition between PDA and PBT at the HF, B3LYP, and second-order many-body perturbation theory [MBPT(2)] levels. All these calculations predict PDA to be more stable than PBT by 28–87 kJ mol⁻¹. A minimum corresponding to the PBT-like structure is found at the HF level, but not at the B3LYP or MBPT(2) level. We report the frequencies of all the infrared- and Raman-active vibrational modes of PDA at the HF and B3LYP levels. The frequencies of the carbon backbone stretching modes calculated at the B3LYP/6-31G* level are within 60 cm⁻¹ of the measured frequencies of resonance Raman bands, when the former values are scaled by a uniform scale factor of 0.96. The ionization potential (IP), electron affinity (EA), and fundamental band gap (E_g) of PDA are calculated at the HF and B3LYP levels and also at the MBPT(2) level employing the quasiparticle formalism. B3LYP/6-31G* provides the most reasonable IP, EA, and E_g , which are within 0.6 eV of the experimental results. Vertical excitation energies to the lowest singlet and triplet excitons of PDA are obtained by configuration interaction singles and by time-dependent density functional theory employing the B3LYP functional. These treatments properly account for the nonvanishing exciton binding energy. While the CIS/6-31G* excessively overestimates the singlet excitation binding energies, B3LYP/6-31G* provides a value (0.3 eV) that is in good agreement with experiment (0.4 eV). © 2001 American Institute of Physics. [DOI: 10.1063/1.1368136]

I. INTRODUCTION

Polydiacetylenes¹ have two unique characteristics. (1) They have fully conjugated π electrons and (2) they can be prepared in single crystal forms when hydrogen atoms on the carbon backbones are substituted with appropriate side groups. These unique characteristics make these polymers ideal systems for experimental investigations and may facilitate commercial applications. By choosing different side groups, one may alter the backbone geometries slightly and thereby control some important chemical and physical properties of the polymers which are associated with the conjugated π electrons. For example, one can synthesize the polydiacetylenes with an acetylenic backbone structure or those with a butatrienic backbone structure (see Fig. 1), and the electronic structures and associated properties would differ accordingly. Despite the presence of bulky side groups, one is still able to study the properties arising primarily from the conjugated π electrons selectively by a number of experimental methods. Optical absorption spectroscopy^{2,3} makes it possible to measure the strong $\pi^* \leftarrow \pi$ transition associated with the backbone π electrons and also the excitonic transitions which primarily involve backbone π electrons but lie

lower than these strong $\pi^* \leftarrow \pi$ transitions. Raman spectroscopy with the excitation laser wavelength tuned into resonance with the $\pi^* \leftarrow \pi$ transition selectively probes the vibrational normal modes of carbon backbones.^{4,5} On the other hand, it is not straightforward to extract electronic and structural information about the carbon backbone from photoelectron spectra⁶ or infrared spectra,⁷ due to the manifold of bands associated with the side groups in these spectra.

A considerable number of theoretical studies have been reported on polydiacetylenes. Among them, a study by Karpfen⁸ offers a comprehensive theoretical account of many properties of the polymers in their ground electronic states. He carried out *ab initio* Hartree–Fock (HF) crystalline orbital (CO) calculations with the STO-3G and $7s3p/3s$ basis sets for the acetylenic and butatrienic structures of unsubstituted polydiacetylene (hereafter simply referred to as PDA and PBT, respectively) and obtained optimized geometries, relative stability of these two isomers, energy band structures, and some selected force constants. Although the calculations employed the first neighbor approximation for the lattice summations and small basis sets, this study provided valuable qualitative information about the structural and energetic properties of the polymer. The next contribution was made by Suhai,⁹ who incorporated the effects of electron correlation via second-order many-body perturbation theory

^{a)}Electronic mail: bartlett@qtp.ufl.edu

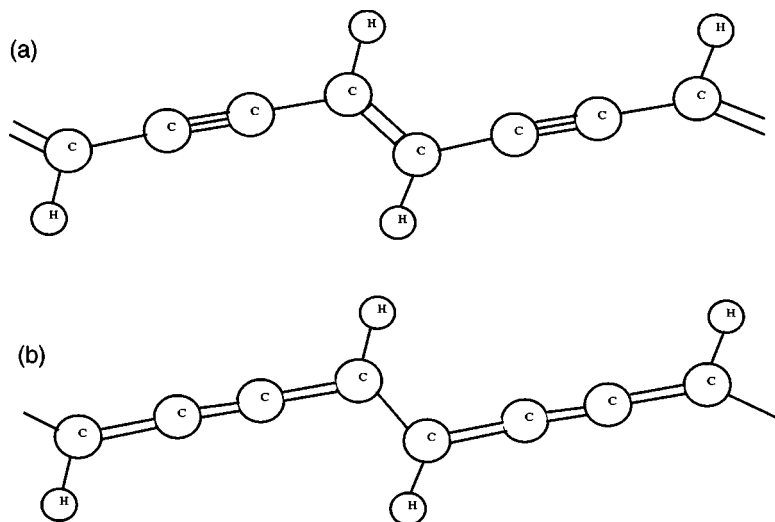


FIG. 1. Structures of the polydiacetylene polymer chains. (a) An acetylenic structure (PDA). (b) A butatrienic structure (PBT).

[MBPT(2)]^{10–12} into the *ab initio* CO calculations. He obtained the total and relative energies, quasiparticle energy bands, and excitation energies to the lowest-lying singlet and triplet excitons for PDA and PBT using STO-3G and 6-31G** basis sets. The excitation energies were calculated with some semiempirical consideration of the screening effects of electron–hole interaction, providing reasonable agreement with the available experimental results. Periodic density functional theory (DFT) calculations employing the $X\alpha$ functional were performed on unsubstituted polydiacetylenes by Boudreaux and Chance.¹³ In contrast to the above-mentioned *ab initio* CO calculations, these DFT calculations failed to provide a qualitatively correct description of the structural and energetic properties of polydiacetylenes, which may be consistent with a similar failure encountered in the application of local DFT to polyacetylenes.^{14–19}

The last 15 years have witnessed a significant advance in the *ab initio* CO theory and periodic linear-combination-of-atomic-orbital (LCAO) DFT of polymers.^{20–23} A robust lattice summation scheme, based on the so-called Namur cutoff criterion and the multipole expansion technique, has been proposed by Delhalle and coworkers,^{24–26} and has made it possible to routinely obtain precise total HF energies of infinite polymers with polar unit cells. Analytical gradients of the HF energy have been formulated and implemented for infinite polymers by Teramae and coworkers²⁷ and have been employed to determine the optimized geometries and vibrational frequencies of infinite polymers efficiently. This has been extended to LCAO DFT for infinite polymers employing local, gradient-corrected, and hybrid functionals by Hirata and Iwata.²⁸ Sun and Bartlett have computed the total energies²⁹ and quasiparticle energy bands³⁰ of infinite polymers at the MBPT(2) level by carefully examining the energy convergence with respect to the lattice summations. Excited-state calculations of polymers have also been made possible with configuration interaction singles (CIS),^{9,31,32} time-dependent HF (TDHF),^{31,32} time-dependent DFT (TDDFT),³² and some approximate many-body Green's-functional (MBGF) theories³³ by employing an efficient direct CI algorithm and a robust lattice summation scheme. These and other methods have been implemented into some

versatile CO program packages,^{29,34–41} and the results obtained from them may be directly compared with the results of molecular orbital (MO) calculations of oligomers obtained from any available MO program packages for the same basis sets.

In light of these advances, we consider it important to apply modern *ab initio* CO and periodic LCAO DFT methods to polydiacetylenes, which are one of the experimentally best-characterized polymers. Such an application will not only provide detailed electronic and structural information about these π -conjugated polymers that may not be obtained from experimental studies, but also help to better estimate the performance of the methods for infinitely extended systems. In this study we perform a series of *ab initio* CO and periodic LCAO DFT calculations for the ground and excited states of polydiacetylenes, and compare the results among themselves and against some available experimental data. Our study is, therefore, along the same direction pursued by Karpfen, Suhai, and others. However, besides the fact that our *ab initio* CO and periodic LCAO DFT calculations are on an equal footing with the *ab initio* MO and LCAO DFT calculations on oligomers, they also offer several new contributions. (1) First, we perform a complete geometry optimization of an infinite chain of PDA (and of PBT, when it exists) with the only constraint arising from the assumption of the C_{2h} symmetry of the polymer. The calculations are carried out efficiently with the aid of the analytical energy gradient technique for *ab initio* HF CO theory and periodic DFT employing the Becke3-Lee-Yang-Parr (B3LYP) hybrid functional. (2) On the basis of these optimized geometries, we compute the relative stability of the two isomers. Potential energy curves along the structural transition between PDA and PBT are also obtained at the HF, B3LYP, and MBPT(2) levels. (3) We then compute the frequencies of the infrared- and Raman-active vibrational modes of the infinite PDA chain at the HF and B3LYP levels at their respective optimized geometries. The force constants in the Cartesian coordinate basis required in the normal coordinate analysis are obtained by numerical differentiation of analytical energy gradients with respect to geometrical displacements. (4) The ionization potential (IP) and electron affinity (EA) of PDA

are also computed in three different approaches: HF, B3LYP, and MBPT(2). The *ab initio* HF CO method and periodic B3LYP DFT provide their IP's and EA's as the negative of the highest occupied orbital (HOMO) and lowest unoccupied orbital (LUMO) energies, respectively, within Koopmans' theorem (or its analogy to DFT). Correlation corrections to Koopmans' IP and EA are computed with the MBPT(2) quasiparticle method. The fundamental band gap, which corresponds to the IP minus EA, is also obtained at the HF, B3LYP, and MBPT(2) levels. (5) The vertical excitation energies to the lowest singlet and triplet excitons of PDA are also computed by the configuration interaction singles (CIS) method and by time-dependent density functional theory (TDDFT) employing the B3LYP functional. Convergence of the calculated vertical excitation energies with respect to the chain length is studied by performing some MO and DFT calculations on oligomers together with the CO and periodic DFT calculations on the polymers. This study offers a comprehensive theoretical account of polydiacetylenes.

II. METHODS OF CALCULATIONS

The geometry optimization of infinite chains of PDA is performed using analytical energy gradients²⁸ for *ab initio* HF CO theory and for periodic DFT employing the B3LYP⁴² functional with the STO-3G, 6-31G, 6-31G*, and 3-21G (Refs. 43–46) basis sets. The geometry of PBT is also optimized at the HF level with the same series of basis sets. The C_{2h} symmetry of these polymers is assumed, as it is unlikely that lifting this symmetry constraint will lead to geometries with lower energies. An attempt to find a local minimum at a

PBT-like structure with the B3LYP functional turned unsuccessful, meaning that PBT is located either at a very shallow local minimum or at a shoulder in the potential energy hypersurface. The geometry optimization procedure is based on a simple steepest descent algorithm with the geometry direct inversion in the iterative subspace (GDIIS) extrapolation of Császár and Pulay.⁴⁷ For infinitely extended systems, the infrared- and Raman-active vibrational modes correspond to the in-phase ($k=0$) motion of nuclei.⁴⁸ We compute the frequencies of these infrared- and Raman-active ($k=0$) vibrational modes by a normal coordinate analysis with the force constants calculated at the HF and B3LYP levels. The force constants are obtained by numerical differentiation of analytical gradients of the energies with the step size of the numerical differentiation being 0.02 Bohr. The evaluation of all the $k=0$ Cartesian force constants involves analytical energy gradient calculations at 15 symmetrically distinct geometries for each theoretical model. The HF and B3LYP single-point energy calculations and analytical energy gradient calculations are performed using a direct algorithm for the integral evaluation. The potential energy curves of the PDA to PBT transition are computed at the MBPT(2) level as well as at the HF and B3LYP levels with the STO-3G basis set at the respective HF/STO-3G optimized geometries. The IP and EA of PDA are computed as the negative of the HOMO and LUMO energies, respectively, at the HF and B3LYP levels. This treatment can be justified by Koopmans' theorem for the IP and EA of HF and by the theorem proven by Levy, Perdew, and Sahni⁴⁹ and by Almbladh and von Barth⁵⁰ for the IP of DFT. The IP and EA are also computed at the MBPT(2) level on the basis of the formula^{12,29,30}

$$\begin{aligned} \epsilon_{p[k_p]}^{\text{MBPT}(2)} = & \epsilon_{p[k_p]}^{\text{HF}} + \sum_j \sum_{a,b} \sum_{k_j, k_b}^{\text{BZ}} \frac{2|(p^{[k_p]} a^{[k_a]} | j^{[k_j]} b^{[k_b]})|^2 - \Re[(p^{[k_p]} a^{[k_a]} | j^{[k_j]} b^{[k_b]}) (p^{[k_p]} b^{[k_b]} | j^{[k_j]} a^{[k_a]})^*]}{\epsilon_{p[k_p]}^{\text{HF}} + \epsilon_{b[k_b]}^{\text{HF}} - \epsilon_{i[k_i]}^{\text{HF}} - \epsilon_{j[k_j]}^{\text{HF}}} \\ & + \sum_{i,j} \sum_b \sum_{k_j, k_b}^{\text{BZ}} \frac{2|(i^{[k_i]} p^{[k_p]} | j^{[k_j]} b^{[k_b]})|^2 - \Re[(i^{[k_i]} p^{[k_p]} | j^{[k_j]} b^{[k_b]}) (i^{[k_i]} b^{[k_b]} | j^{[k_j]} p^{[k_p]})^*]}{\epsilon_{p[k_p]}^{\text{HF}} + \epsilon_{b[k_b]}^{\text{HF}} - \epsilon_{i[k_i]}^{\text{HF}} - \epsilon_{j[k_j]}^{\text{HF}}}, \end{aligned}$$

where i and j represent occupied orbitals, a and b virtual orbitals by convention, and ϵ^{HF} and $\epsilon^{\text{MBPT}(2)}$ are the orbital energies of the respective theoretical levels. For the definition of the wave-vector-dependent two-electron integrals, see, e.g., Ref. 33. The wave vectors, which are denoted by k , satisfy the following relations

$$k_p + k_j = k_a + k_b + \frac{2m\pi}{R_t}, \quad (1)$$

$$k_i + k_j = k_p + k_b + \frac{2n\pi}{R_t}, \quad (2)$$

where R_t represents the translational period and m and n are integers. These expressions are well-defined only when the corresponding HF orbital energies are in the energy range given by

$$\epsilon_{\text{HOMO}}^{\text{HF}} - E_g^{\text{HF}} < \epsilon_{p[k_p]}^{\text{HF}} < \epsilon_{\text{LUMO}}^{\text{HF}} + E_g^{\text{HF}}, \quad (3)$$

where E_g^{HF} is the HF fundamental band gap. The highest occupied and lowest unoccupied HF orbitals are always within this range and hence Eqs. (1) and (2) are well-defined for our purpose. The MBPT(2) singlepoint energy calculations and quasiparticle energy calculations are accomplished with disk-based algorithms. The vertical excitation energies to the lowest singlet and triplet exciton states of PDA are computed by CIS^{9,31,32} and TDDFT³² using the B3LYP functional. We invoke the trial-vector algorithms proposed by Davidson⁵¹ and modified by others^{52–55} such that the atomic-orbital (AO)-based two-electron integrals are never stored, but recomputed as needed and the transformation of these integrals from the AO basis to the CO basis is avoided.³²

All the *ab initio* CO and periodic DFT calculations are

TABLE I. Optimized geometrical parameters of an infinite chain of polydiacetylene in an acetylenic structure (PDA) obtained by *ab initio* HF CO theory and periodic DFT employing B3LYP functional. Bond lengths are given in Å and bond angles in degrees.

Theory	$r_{C\equiv C}$	$r_{C=C}$	r_{C-C}	r_{C-H}	$a_{C=C-C}$	a_{H-C-C}	$a_{C\equiv C-C}$
HF/STO-3G	1.178	1.328	1.448	1.086	123.4	116.4	179.7
HF/3-21G	1.193	1.331	1.422	1.073	123.1	116.7	179.4
HF/6-31G	1.200	1.337	1.424	1.074	123.7	116.5	178.7
HF/6-31G*	1.193	1.331	1.430	1.075	123.2	116.7	178.4
B3LYP/STO-3G	1.221	1.375	1.432	1.103	123.5	117.2	179.4
B3LYP/3-21G	1.221	1.366	1.400	1.088	123.7	117.4	179.2
B3LYP/6-31G	1.228	1.371	1.403	1.089	124.2	117.3	178.5
B3LYP/6-31G*	1.224	1.368	1.401	1.089	123.9	117.4	178.1
HF/7s3p/3s ^a	1.194	1.321	1.425	(1.087)	(123.9)	(115.3)	(180.0)
Experiment ^b	1.19	1.36	1.43		121.9	115.8	177.6
Experiment ^c	1.21	1.33	1.44		120.9	120.1	174.4
Experiment ^d	1.21	1.36	1.41				

^aReference 8. The numbers in parenthesis are not optimized.

^bReferences 60 and 61.

^cReference 62.

^dReference 59.

performed with the POLYMER⁴¹ program, which employed the so-called Namur cutoff criterion^{24,25} for truncating the infinite lattice summations (see Ref. 56 for the performance of various cutoff criteria). The cutoff radius for the short-range lattice summations (i.e., those for the overlap integrals, the kinetic integrals, and the overlap-like lattice summations of the nuclear-attraction and two-electron integrals) is sufficiently large, so that the lattice sums are practically converged. The long-range lattice summations (i.e., those for the r_{12}^{-1} interactions of the nuclear attraction and two-electron integrals) are truncated after ten unit cells (one unit cell contains four carbon atoms and two hydrogen atoms) on both sides of the reference unit cell for the HF, B3LYP, and MBPT(2) calculations. It is generally necessary to take a larger cutoff radius in excited-state calculations.³² We include 20 unit cells on both sides of the reference unit cell for the long-range lattice summations in the CIS and TDDFT calculations. We use 30 evenly spaced wave-vector sampling points for the HF, B3LYP, and MBPT(2) calculations and 40 for the CIS and TDDFT calculations. The multipole expansion technique is not invoked in this study, as the unit cell does not have a permanent dipole. The HF and B3LYP calculations on oligomers of PDA are performed by using the ACES II⁵⁷ and Q-CHEM⁵⁸ programs. The structures of these oligomers are obtained by simply repeating the optimized geometries of the unit cell of the infinite chains obtained at the respective theoretical levels and attaching some appropriate end groups.

III. RESULTS AND DISCUSSION

A. Equilibrium structure

The optimized geometrical parameters and some available experimental data of PDA are presented in Table I. The experimental data were obtained for substituted polydiacetylenes in PDA-like structures, and hence may not be compared straightforwardly with the calculated results for unsubstituted PDA. Indeed, the polydiacetylenes with different side groups have slightly different geometries, although they

all correspond to the PDA-like structures. For example, the measured C≡C bond length varies in the range of 1.19–1.21 Å,^{59–62} depending on the side groups. Similarly, the measured C=C and C–C bond lengths are in the range of 1.33–1.36 and 1.41–1.44 Å,⁶³ respectively, and there is also some variation in the experimental results of bond angles.

The calculated geometric parameters appear to converge rapidly with increasing basis set size. The HF/6-31G* and B3LYP/6-31G* values may be considered to be practically converged with respect to the basis set size and it is possible to draw definitive conclusions on the performance of these methods on the geometry. Overall, the equilibrium bond lengths computed from the HF/6-31G* and B3LYP/6-31G* calculations are in good agreement with the experimental data. For example, the calculated C≡C bond lengths at the HF/6-31G* and B3LYP/6-31G* levels (1.19 and 1.22 Å) are consistent with the measured bond lengths (1.19–1.21 Å). The calculated C=C (1.33 and 1.37 Å) and C–C bond lengths (1.43 and 1.40 Å) at the HF/6-31G* and B3LYP/6-31G* levels are also embraced in the range of the corresponding experimental bond lengths. The variation in the experimental bond angles is ~4°. Considering that this variation likely arises from the effects of bulky side groups and their crystal packing, the agreement between the calculated and observed bond angles is reasonable. We also note that the bond lengths optimized by Karpfen at the HF/7s3p/3s level with fixed bond angles are consistent with our optimized geometrical parameters obtained at the HF/3-21G level (the 7s3p/3s basis set is similar to the 3-21G basis set in size).

As noted by Karpfen and also evident from Table I, owing to the delocalized nature of the conjugated π electrons, the C≡C, C=C, and C–C bonds in PDA assume substantial C=C, C–C, and C=C bonding character, respectively. For example, the calculated and observed C≡C bond lengths of PDA are appreciably longer than the isolated (nonconjugated) C≡C bond in acetylene (1.17 Å), indicating the appreciable C=C bonding character in the former. Likewise, the C=C and C–C bonds of PDA are longer and

TABLE II. Optimized geometrical parameters of an infinite chain of polydiacetylene in a butatrienic structure (PBT) obtained by *ab initio* HF CO theory. Bond lengths are given in Å and bond angles in degrees.

Theory	$r_{\text{C}=\text{C}}$	$r_{\text{C}-\text{C}}$	$r_{\text{HC}=\text{CC}}$	$r_{\text{C}-\text{H}}$	$\alpha_{\text{C}-\text{C}=\text{C}}$	$\alpha_{\text{H}-\text{C}=\text{C}}$	$\alpha_{\text{C}=\text{C}=\text{C}}$
HF/STO-3G	1.245	1.473	1.314	1.087	123.6	119.9	179.9
HF/3-21G	1.249	1.451	1.314	1.074	123.2	119.4	179.8
HF/6-31G	1.256	1.449	1.322	1.075	123.7	119.1	179.9
HF/6-31G*	1.255	1.453	1.317	1.076	123.3	119.2	180.0
HF/7s3p/3s ^a	1.248	1.468	1.319	(1.087)	(123.7)	(119.4)	(180.0)
Experiment ^b	1.29	1.42	1.38		119.2	116.0	177.2

^aReference 8. The numbers in parenthesis are not optimized.

^bReference 63.

shorter, respectively, than the C=C bond in ethylene (1.31 Å) and the C-C bond in ethane (1.54 Å). In the language of valence bond theory, the electronic structure of PDA is a mixture of the two valence bond structures, the PDA type and the PBT type, depicted in Figs. 1(a) and 1(b), respectively, with the PDA-type structure being dominant. Even at the HF level, in which the electron correlation effects are not taken into account, the ground-state wave function of PDA is a mixture of these two valence bond structures, and hence it properly accounts for the mixed single, double, and triple bond orders in PDA. As the electron correlation effects are taken into account, the ground-state wave function of PDA will have an increased proportion of the PBT-type valence bond structure. This may be understood by remembering that the HOMO has the PDA-type bonding pattern and the LUMO has the PBT-type bonding pattern and the inclusion of electron correlation effects amounts to including the determinants, in which electrons are promoted from the HOMO to the LUMO. Thus we can expect that the C≡C bond will have greater C=C bond character and likewise the C=C and C-C bonds will have greater C-C and C=C bond character, ongoing from HF to a correlated method. Indeed, we observe the expected changes in the CC bond lengths ongoing from the HF to B3LYP results, although the latter is not a conventional wave-function-based correlation treatment. For example, C≡C and C=C bonds lengthen by ~0.03 Å, while the C-C bond shortens by ~0.03 Å, ongoing from the HF to B3LYP method. Essentially the same phenomenon has been observed in the optimized geometries of polyacetylenes.¹² This phenomenon also manifests itself in the calculated vibrational frequencies and is discussed in Sec. III C.

In Table II we list the geometric parameters of PBT optimized at the HF level with different basis sets. The B3LYP calculation failed to locate a local minimum of PBT, details of which are discussed in Sec. III B. We again observe that the optimized geometries of PBT exhibit rapid convergence with respect to the basis set size and hence the HF/6-31G* result is considered to be sufficiently close to the HF limit. We also note that the optimized geometry of Karpfen obtained from the HF/7s3p/3s calculation is consistent with the result of our HF/3-21G calculation. From Tables I and II we find that the agreement between the calculated and measured geometric parameters is less satisfactory for PBT than for PDA. For example, the calculations tend to underestimate C=C bond lengths and overestimate the C-C bond

lengths by 0.03–0.06 Å. The larger deviation between the calculated and measured geometric parameters of PBT may partly be ascribed to the effects of bulky side groups and of crystal packing on the experimental result. These effects are probably greater on PBT structures than on PDA structures because it is the bulky side groups that prevent PBT, which is a local minimum, from relaxing to PDA, which is the global minimum, in the course of polymer synthesis and crystallization. However, for the same reason that PBT is a local minimum, the accurate description of the potential energy hypersurface near PBT will be computationally demanding, and it is possible that the HF description of PBT is slightly worse than that of PDA. Nevertheless, in spite of the above-mentioned deviation, the calculations reproduce the bonding pattern and other qualitative structural characteristics of PBT correctly. We add that our optimized geometries of PDA and PBT at the HF/6-31G level are in excellent agreement with those obtained from an oligomer extrapolation method employing an independent program.⁶⁴

B. Energetics

Figure 2 is a plot of the potential energy curves along the PDA to PBT transition at the HF level with the STO-3G, 3-21G, 6-31G, and 6-31G* basis sets. The horizontal axis (Δ) refers to the fraction of the PBT structural parameters. Geometrical parameters are generated by linear interpolation of the optimized PDA and PBT structures to calculate the potential energy curve. The calculations are performed at Δ being equal to 0.0 (PDA), 0.2, 0.4, 0.6, 0.8, and 1.0 (PBT). We do not obtain a converged result at $\Delta=0.8$ with the 3-21G basis set because of the oscillations of the density matrix between the PDA-like and PBT-like electronic configurations. In other words, there is a HOMO-LUMO crossing around $\Delta=0.8$ in the HF/3-21G curve as previously suggested by Karpfen⁸ and by Whangbo *et al.*⁶⁵

Karpfen calculated a potential energy curve along the PDA to PBT transition using the STO-3G basis set within the first- to third-neighbor approximations and using the 7s3p/3s basis set within the first-neighbor approximation. His result is consistent with ours; the relative stability of PDA over PBT at the HF/STO-3G level is 83.7 kJ/mol⁻¹ by Karpfen and is 87.0 kJ/mol⁻¹ from our calculation which includes ten neighbor unit cells. The relative stability at the HF/7s3p/3s level is 50.2±4.2 kJ/mol⁻¹ (Karpfen), which compares well with our HF/3-21G result, 48.2 kJ/mol⁻¹. The

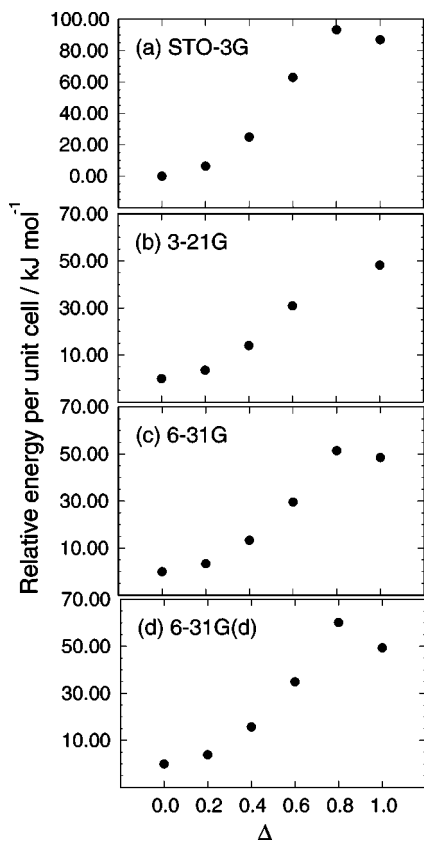


FIG. 2. The ground-state potential energy curves along the structural transition between PDA and PBT computed at the HF/STO-3G, HF/3-21G, HF/6-31G, and HF/6-31G*. $\Delta=0$ corresponds to the PDA structure and $\Delta=1$ to the PBT structure optimized at each basis set. The total energy of the PDA at each basis set is taken as the reference energy.

energy barrier for the PDA to PBT transition appears to be only slightly larger than the relative energy. In other words, the minimum for the PBT structure is very shallow toward PDA. A rough estimate of the energy barrier relative to PDA is obtained as the energy difference between $\Delta=0$ and $\Delta=0.8$, and is 60 kJ mol^{-1} at the HF/6-31G* level. Though the geometry optimization of the transition state would lower the barrier, this value is consistent with an experimental finding by Wegner,² who reported that the experimental energy barriers were between $58\text{--}97 \text{ kJ mol}^{-1}$ depending on side groups. Suhai⁹ also reported the relative stability at the HF and second-order Møller–Plesset perturbation theory [MPPT(2)] levels using the STO-3G and 6-31G** basis sets. His calculated values 47.8 , 37.0 , 34.4 , and 24.0 kJ mol^{-1} for HF/STO-3G, HF/6-31G**, MPPT(2)/STO-3G, and MPPT(2)/6-31G** are significantly lower than ours. Since geometries in his calculations were taken from experimental structures of substituted polydiacetylenes and the calculations were performed by simply substituting side groups by hydrogen atoms, the PDA-like and PBT-like structures used were not at the minima of the potential energy surface.

The relative stability calculated with the STO-3G basis set is substantially larger than the value obtained with 3-21G, 6-31G, and 6-31G* basis sets (48.2 , 49.5 , and 49.4 kJ mol^{-1} , respectively). These numbers seem to be converged with respect to the basis set size and are considered as the HF limit

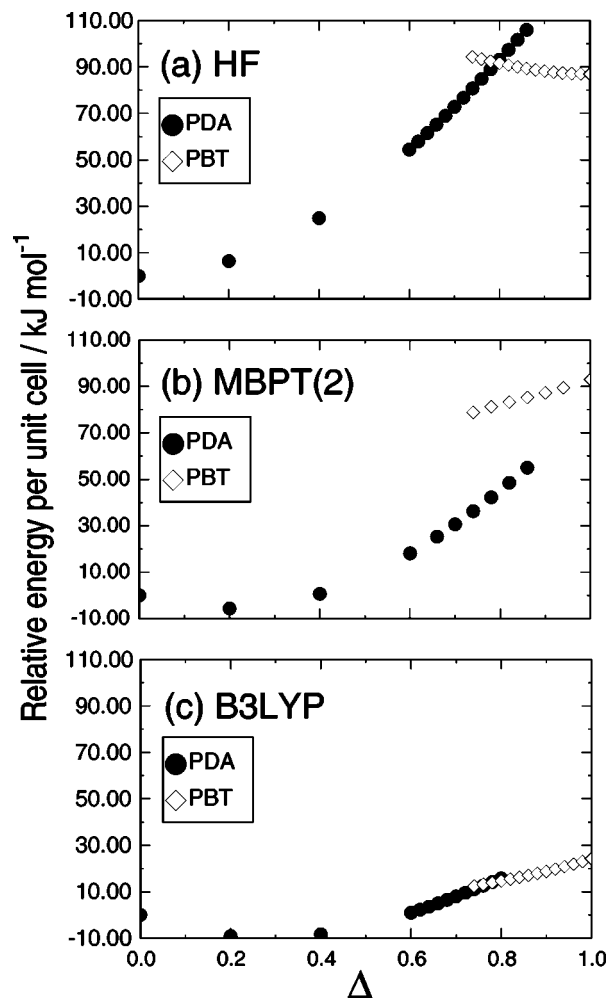


FIG. 3. Potential energy curves along the structural transition between PDA and PBT computed at the HF/STO-3G, B3LYP/STO-3G, and MBPT(2)/STO-3G levels. $\Delta=0$ corresponds to the PDA structure and $\Delta=1$ to the PBT structure optimized at HF/6-31G*. The total energy of the PDA at each theoretical level is taken as the reference energy. The black closed circle plots are energy of PDA type wave function and open diamond plots are energy of PBT wave function.

results. Interestingly, we obtain a converged relative energy already with the 3-21G basis set, which is usually too small in molecular calculations. This is one of the characteristics of the calculations of infinitely extended systems. As the tails of the basis functions from the neighbor unit cells can contribute to the central unit cell, the description of the long range region of the basis functions in the central unit cell is well-complemented by basis functions of the neighbor unit cells, making the calculations converge to the basis set limit rapidly.

Figure 3 is a plot of the potential energy curve along the PDA to PBT transition computed at HF/STO-3G, MBPT(2)/STO-3G//HF/STO-3G, and B3LYP/STO-3G//HF/STO-3G levels. The Δ between 0.6 and 1.0 are taken at a 0.02 step size in HF and B3LYP calculations. Each energy calculation is performed with an initial density as one that is converged in a previous geometry so that we stay on the wave function of interest. The MBPT(2) energy calculation is performed at Δ equal to 0.60, 0.66, 0.70, 0.74, 0.78, 0.82, 0.86, 0.90, 0.94, and 1.00 as well as 0.00, 0.20, and 0.40. Notice that the

TABLE III. Frequencies of $k=0$ vibrational modes (in cm^{-1}) of an infinite chain of polydiacetylene in an acetylenic structure (PDA).

Mode	Experiment ^a	HF				B3LYP				
		STO-3G	3-21G	6-31G	6-31G*	STO-3G	3-21G	6-31G	6-31G*	
a_g	ν_1		3710	3351	3361	3374	3422	3159	3167	3165
	ν_2	2098	2771	2501	2486	2494	2350	2204	2188	2176
	ν_3	1490	1960	1783	1801	1806	1633	1532	1549	1540
	ν_4	1204	1526	1468	1467	1445	1370	1323	1328	1305
	ν_5	955	1077	1050	1043	1023	967	957	958	945
	ν_6		535	528	502	475	436	417	416	415
b_u	ν_7		3694	3359	3366	3378	3418	3170	3176	3173
	ν_8		1503	1455	1458	1431	1407	1383	1402	1395
	ν_9		1381	1313	1347	1321	1307	1298	1302	1269
	ν_{10}		500	496	490	477	454	454	452	447
a_u	ν_{11}		1189	1116	1117	1099	1028	983	989	972
	ν_{12}		504	487	486	470	431	420	428	424
b_g	ν_{13}		1022	1055	1039	971	865	890	903	858
	ν_{14}		522	606	581	488	436	463	471	467

^aReference 68.

inclusion of electron correlation alters the shape of the potential energy curves qualitatively. The B3LYP does not predict a double minima corresponding to PDA and PBT, but only a single minimum at the PDA structure. There is a shoulder where PBT would have been expected. Likewise MBPT(2), though a strong function of its HF reference, still predicts a flatter PDA potential curve, and the ground-state curve exhibits a discontinuity where the HF curves cross. In both correlated treatments, the sign of the slope in the PBT wave-function curves is reversed from that of the HF curve. From these results we conclude that electron correlation strongly disfavors the PBT structure. However, considering the fact that the basis set employed here is small and the geometry is not optimized at each point of the potential energy curves, the reliability of the MBPT(2)/STO-3G and B3LYP/STO-3G results must not be overrated. There are some experimental data⁶⁶ that indicate the existence of a PBT minimum on the potential energy surface, which might be partly due to polydiacetylene having bulky side groups. It is also possible that the MBPT(2)/STO-3G and B3LYP/STO-3G potential energy curves, which do not have a PBT minimum, are qualitatively wrong, or qualitatively different, from curves which would be obtained with the optimized geometry at each point that corresponds to a theoretical level using large basis sets, although this does not appear likely. Note that pure DFT calculations fail to describe the potential energy curve along the bond alternation coordinate qualitatively correctly.⁶⁷

C. Vibrational frequencies

For an infinite crystalline system, the vibrational modes which give rise to infrared and Raman bands occur at the center ($k=0$) of the Brillouin zone of the phonon dispersion curves, owing to the momentum conservation law.⁴⁸ The calculated harmonic frequencies of all the $k=0$ vibrational modes of PDA obtained from the HF and B3LYP methods are given in Table III. The vibrational modes are categorized into a_g , b_u , a_u , or b_g irreducible representations as the unit

cell of PDA belongs to the C_{2h} point group. Among them, only some of the a_g vibrations are unambiguously assigned to the observed bands,⁶⁸ as they give rise to intense bands in resonance Raman spectra with the incident laser wavelength tuned into resonance with the $\pi^* \leftarrow \pi$ electronic transition. These a_g vibrations involve, to a varied degree, the stretching and bending motion of the carbon backbone and strongly modulate the π -electronic structure of PDA. Infrared spectroscopy, on the other hand, tends to provide complex spectra that are dominated by the bands from the side groups,⁷ and it is not straightforward to identify the bands associated with the PDA carbon backbone.

The calculated frequencies converge with respect to the basis set size smoothly and rather rapidly at the corresponding limiting values. As is well-known, these calculated frequencies obtained from the HF and B3LYP calculations are higher than the observed frequencies. Universal scale factors were determined by Scott and Radom⁶⁹ and by Wong⁷⁰ from a least-squares fitting procedure to a set of a large number of calculated and observed frequencies. They are 0.9613 (Ref. 69) or 0.9614 (Ref. 70) for the B3LYP/6-31G* and 0.8953 (Ref. 70) for the HF/6-31G*. Scaling the frequencies of PDA obtained from the B3LYP/6-31G* calculations by the recommended scale factor (0.9614), we find that the calculation and experiment agree with each other reasonably well. The scaled B3LYP/6-31G* frequencies are 2092, 1481, 1255, and 909 cm^{-1} for the observed bands⁶⁸ at 2098, 1490, 1204, and 955 cm^{-1} , respectively. The agreement is less satisfactory for the HF/6-31G* frequencies after they are scaled by 0.8953. The scaled HF/6-31G* frequencies are 2233, 1617, 1294, and 916 cm^{-1} . The scaled calculated frequencies for ν_2 and ν_3 modes are significantly overestimated and the deviations are as large as $\sim 120 \text{ cm}^{-1}$, indicating that the raw HF frequencies of ν_2 and ν_3 of PDA are particularly overestimated relative to the other raw HF frequencies. We believe that this is not accidental, as a similar trend has been observed for another important conjugated π -electron polymer, i.e., polyacetylene.^{71,72} It has been found that the elec-

TABLE IV. The ionization potential (IP), electron affinity (EA) and band gap (E_g) (in eV) of an infinite chain of polydiacetylene in an acetylenic structure (PDA). The IPs and EAs are calculated at the HF and B3LYP levels at the respective optimized geometries as the negatives of the highest occupied and lowest unoccupied orbital energies, respectively, according to Koopmans' theorem and its DFT variant. The MBPT(2) calculations of the IPs and EAs are based on the HF optimized geometries and the frozen core approximation. The fundamental band gaps correspond to (IP-EA).

	IP	EA	E_g
HF/STO-3G	5.92	-3.95	9.87
HF/3-21G	7.36	-0.42	7.78
HF/6-31G	7.18	-0.50	7.68
HF/6-31G*	7.33	-0.67	8.00
B3LYP/STO-3G	3.39	0.86	2.53
B3LYP/3-21G	4.99	3.20	1.78
B3LYP/6-31G	4.84	3.12	1.72
B3LYP/6-31G*	4.83	3.15	1.68
MBPT(2)/STO-3G	5.49	-3.53	9.03
MBPT(2)/3-21G	6.75	0.70	6.05
MBPT(2)/6-31G	6.54	0.65	5.89
Experiment	5.5±0.1 ^a , 5.2±0.1 ^b , 5.8 ^c	3.1±0.1 ^a , 3.4 ^c	~2.4 ^a

^aReference 76.

^bReference 75.

^cReference 74.

tron correlation effect is particularly large on the calculated frequency of the so-called "in-phase C=C stretching mode" (Ref. 71) or "bond order alternating mode" (Ref. 72), which gives rise to an intense Raman band, and that the HF frequencies of this mode tend to be excessively overestimated even after the simple scaling procedure proposed by Pulay.⁷³ Since the in-phase C=C stretching mode is a simultaneous C=C bond stretch and C-C bond shrinkage and the HOMO of this polymer has the C=C bonding and C-C antibonding character and the LUMO has the C=C antibonding and C-C bonding character, the in-phase C=C stretching mode strongly couples with the energy levels of the HOMO and LUMO. The calculated frequency of this mode is particularly sensitive to the treatment of electron correlation, as the latter includes the determinant in which electrons are promoted from the HOMO to the LUMO into the wave function. We consider that the same argument explains the overestimation of the scaled frequencies of ν_2 and ν_3 of PDA at the HF level. The normal coordinates of these modes are along the transition between PDA and PBT, and hence the vibrational motion along them couples with the energy levels of the HOMO, which has the PDA-type bonding character, and of the LUMO, which has the PBT-type bonding character. The effect of electron correlation is, therefore, significant on the frequencies of ν_2 and ν_3 . The B3LYP method improves the calculated frequencies of ν_2 and ν_3 remarkably well, as it approximately takes the effects of the electron correlation into account.

D. Ionization potential, electron affinity, and fundamental band gap

The IP, EA, and E_g of PDA calculated by the HF, B3LYP, and MBPT(2) levels are listed in Table IV. The calculations are performed at the HF and B3LYP level with the STO-3G, 3-21G, 6-31G, and 6-31G* basis sets at the

optimized geometries of the respective models and the MBPT(2) level with the STO-3G, 3-21G, and 6-31G basis sets at the HF optimized geometries of the respective basis sets. The IPs calculated at the HF level (i.e., by Koopmans' approximation) appear converged at the limiting value of 7.3 eV. We consider that the inclusion of diffuse basis functions would lead to only a slight change (in the order of a few tenths of an electron volt) in the calculated IPs for the following two reasons. First, this ionization process involves the HOMO, which is expected to have valence character and is spatially compact, and hence the 6-31G* basis set provides a reasonably good description of the process. Second, we have calculated the IPs of an oligomer of PDA (consisting of two C₄H₂ unit cells plus some appropriate end groups) at the HF level across the 6-31G*, 6-31+G*, and 6-31++G** basis sets. We found that the difference in the calculated IP's between the 6-31G* and 6-31++G** basis sets is 0.19 eV, which we consider to be reasonably small.

The IP calculated at the HF/6-31G* (7.33 eV) is noticeably larger than the experimental values, which are in the range of 5 to 6 eV.⁷⁴⁻⁷⁶ Ongoing from the HF to MBPT(2) level, the calculated value of the IP shifts toward the direction of the experimental value. The IP calculated at the MBPT(2)/6-31G level is 6.53 eV, which is more than 0.7 eV higher than one of the experimental values, but the inclusion of electron correlation at this level accounts for a respectable portion of the deviation between the Koopmans' and experimental IPs. Part of the remaining deviation may be ascribed to the polarization or screening effects in the actual three-dimensional polydiacetylene crystals,^{77,78} which are expected to lower the IP. Interestingly, a reasonable value of the IP can be obtained from the B3LYP/6-31G* method (4.83 eV), which is only 0.4 eV lower than one of the experimental values (5.2 eV). As we mentioned already, the HF method overestimates the IP of PDA, whereas DFT tends to underestimate the IP, owing to the unphysically rapid asymptotic decay of the DFT exchange potentials.⁷⁹⁻⁸¹ As the B3LYP functional is a hybrid of the HF exchange (20%) and other approximate exchange and correlation functionals, this error is partly eliminated, making IPs a result of cancellation of a positive error in the HF and a negative error in the DFT. The similar agreement in the IPs between the B3LYP and experimental results has been observed for trans-polyethylene³² and trans- and cis-polyacetylene.⁶⁷

The accurate calculations of EAs are generally much more demanding than those of IPs. The electron-attached states (or the virtual orbitals involved) tend to have a large spatial spread, and diffuse basis functions would be required to describe those states. It is also known that Koopmans' theorem performs poorly for EAs. The EA of PDA computed by the HF/6-31G* method has the wrong sign; the calculated value is -0.67 eV, whereas the experimental value is 3.1-3.4 eV.^{74,76} The LUMO of PDA is primarily of valence character and hence the necessity of diffuse basis functions is relatively small (e.g., compared with the LUMO of polyethylene). Nonetheless, the inclusion of diffuse functions is expected to further increase the EA obtained with the 6-31G* basis set by 0.51 and 0.69 eV, estimated by the oligomer calculations with the 6-31+G* and 6-31++G** basis set,

respectively. Thus Koopmans' approximation excessively underestimates the EA of PDA. The inclusion of electron correlation at the MBPT(2) again corrects the Koopmans' EA toward the direction of the experimental data. However, the calculated value of the EA obtained from the MBPT(2)/6-31G level is 0.65 eV, which is still too small compared to experiment even after adding the basis set correction of 0.69 eV. We also compare the negative of the LUMO energy obtained from the B3LYP calculations (in analogy to Koopmans' theorem for HF) with the experimental EA. The EA from the B3LYP/6-31G* method is 3.15 eV, which is in good agreement with the experimental values. Although the calculated value may change to some extent upon inclusion of diffuse basis functions and the polarization or screening effects of crystals, it appears to be a considerable improvement over HF or even MBPT(2). The much higher value of EA in the B3LYP than in the HF, in other words, a much lower LUMO energy in B3LYP than in the HF, can be traced back to the "multiplicative" nature of the exchange potentials of DFT in contrast to the "orbital-dependent" nature of the HF exchange potential. The HF exchange potential for an occupied orbital comes from the $N-1$ electrons in all the other occupied orbitals, whereas the HF exchange potential for a virtual orbital comes from all the N electrons. The DFT exchange potential, which is seldom accomplished without introducing an "exact exchange" treatment,⁸² on the other hand, is the same for both, if the self-interaction is properly eliminated. Nonetheless, the virtual orbitals of DFT generally lie lower than those of HF, because an electron in a virtual orbital of DFT feels the repulsive interactions from one less electron than does an electron in a virtual orbital of HF. However, the above argument also suggests that it may not be theoretically justifiable to view the negative of the LUMO energy as an approximation to the EA.

Computationally, E_g amounts to the calculated value of (IP-EA) listed in Table IV for each of the theoretical models employed here. As the HF overestimates IP and underestimates EA, we expect that it would excessively overestimate $E_g = \text{IP} - \text{EA}$. Indeed, the HF/6-31G* predicts the value of E_g to be 8.00 eV, which is unreasonably larger than an experimental value (~ 2.4 eV) obtained for a substituted polydiacetylene.⁷⁶ This large error is ascribed to both the approximation in the calculation (inadequacy of the basis set and the neglect of electron correlation) and the polarization or screening effects in the actual material. The inclusion of the effects of electron correlation at the MBPT(2)/6-31G level accounts for a respectable amount (35%) of the error between the HF/6-31G and experimental results. However, the calculated E_g (5.89 eV) is still substantially overestimated compared with the experiment (2.4 eV). The B3LYP calculations again provide the most reasonable result (1.69 eV) of E_g , although it is slightly smaller than the experiment. The agreement is due to the multiplicative nature of the exchange potential of DFT, which also leads to a rather good agreement between the calculated and observed EAs (see above). As mentioned earlier, this characteristic of the exchange potential, however, suggests that it may not be entirely justifiable to consider the energy difference between the HOMO and LUMO of DFT as representing E_g , which

TABLE V. The vertical excitation energies (in eV) to the lowest-lying singlet and triplet excitons of an infinite chain of polydiacetylene in an acetylenic structure (PDA). Excitation energies are calculated by configuration interaction singles (CIS) on the basis of *ab initio* HF CO theory and by time-dependent DFT (TDDFT) employing the B3LYP functional at the respective optimized geometries.

	Singlet	Triplet
HF/CIS/STO-3G	5.34	2.28
HF/CIS/3-21G	3.68	1.82
HF/CIS/6-31G	3.60	1.73
HF/CIS/6-31G*	3.69	1.91
B3LYP/TDDFT/STO-3G	2.25	1.08
B3LYP/TDDFT/3-21G	1.51	0.79
B3LYP/TDDFT/6-31G	1.45	0.77
B3LYP/TDDFT/6-31G*	1.40	0.68
Experiment	2.0 ^{a,b}	

^aReference 5.

^bReference 86.

may be experimentally measured as IP-EA. Indeed, the formal theoretical argument indicates that the HOMO-LUMO energy difference in DFT and the experimental E_g differ from each other by the so-called "discontinuity constant."⁸³⁻⁸⁵ The discontinuity constant accounts for the jump in the exchange potential upon addition of an electron to the system, as the exchange potential in DFT itself is an analytic function of electron density and is not normally capable of exhibiting such a discontinuity upon increasing the number of electrons. Thus generally, the HOMO-LUMO energy difference in DFT is found to be smaller than E_g . The B3LYP functional is a hybrid of HF exchange (20%), conventional exchange and correlation functionals, and hence the overestimation of E_g by HF and the underestimation of E_g by pure DFT, when E_g is approximated as the HOMO-LUMO energy difference, partly cancel each other. Consequently, the HOMO-LUMO energy difference of B3LYP is a reasonable approximation to E_g . It is notable that this hybrid HF and DFT method, B3LYP, which was originally designed to reproduce the experimental thermochemical quantities accurately, does not only provide accurate geometrical parameters and vibrational frequencies of PDA, but also reproduces the IP, EA, E_g , and the excitation energies or exciton binding energies (see below) uniformly better than HF or MBPT(2).

E. Excitation energies to the singlet and triplet excitons

In Table V we compile the calculated vertical excitation energies to the lowest singlet and triplet exciton states of PDA. The calculations are carried out at the CIS and TDDFT (with the B3LYP functional) level employing the STO-3G, 3-21G, 6-31G, and 6-31G* basis sets at their respective optimized geometries. Analogous to polyacetylene,²⁹ the experimental optical absorption band edge of a substituted polydiacetylene is located at ~ 2.0 eV,^{5,86} which is lower than the photoconduction threshold 2.4 eV⁷⁶ and the photoemission threshold 5.5 eV.⁸⁷ This result indicates that the optical absorption at around 2.0 eV is associated with the singlet exciton states that lie below the conduction band. The

wave functions of these exciton states are more suitably described as a linear combination of several singly substituted determinants rather than as one determinant in which an electron is promoted from the HOMO to LUMO. CIS and TDDFT when combined with an appropriate exchange(-correlation) functional are among the simplest excited-state methods that allow the singly substituted determinants of interacting units to mix and provide an appropriate zeroth-order description of the exciton states.

The calculated CIS and TDDFT excitation energies seem converged at 3.7 and 1.4 eV for the singlet exciton state and at 1.9 and 0.7 eV for the triplet exciton state, respectively. However, the excitation energies can be sensitive to the basis set size as is the EA since they are dependent on the quality of the virtual orbitals, and can undergo some further change upon inclusion of diffuse basis functions. We examine this point by performing the CIS calculations for the oligomer (containing two C_4H_2 units and end groups) with the 6-31G*, 6-31+G*, and 6-31++G** basis sets, and find that the lowest singlet and triplet excitation energies are almost converged at the 6-31G* basis set. Singlet energies are 4.88, 4.74, and 4.74 eV and triplet energies are 2.31, 2.31, and 2.31 eV, respectively, in the order of increasing the basis set size. Therefore the lowest singlet and triplet exciton state are characterized as valence excited states. It is established that TDDFT employing current approximate functionals (e.g., Slater functional, Becke88 functional, and the combinations thereof, including B3LYP) tend to give excessively low excitation energies to some excited states, when the excitation energies are close to or higher than the negative of the HOMO energy. This is a consequence of the fact that these functionals give rise to an exchange (exchange-correlation) potential that decays too rapidly (exponentially as opposed to the correct $-r^{-1}$ behavior) in the asymptotic region.⁷⁹⁻⁸¹ For PDA, the negative of the HOMO energy is considerably higher than the excitation energies, so this problem will not manifest itself.

First, we note that both CIS and TDDFT with the B3LYP functional properly account for the positive exciton binding energies, i.e., E_g minus the vertical excitation energies, for both the singlet and triplet excitons. The CIS/6-31G* yields the lowest excitation energy to the singlet exciton (3.7 eV) which is much higher than the experimental value (~ 2.0 eV). Considering that E_g computed by the HF/6-31G* is higher than the experimental data by as much as 5.6 eV, the error (1.7 eV) in the CIS/6-31G* excitation energy to the singlet exciton appears to be moderate. This may be ascribed to the inadequacy of the basis set; the electron-attached state of PDA may be much more diffuse than the valence excited state. The TDDFT calculations with the B3LYP/6-31G* model apparently provide much improved excitation energies. The calculated excitation energy to the singlet exciton (1.4 eV) is lower than the experimental value (~ 2.0 eV), but the agreement between these two values is remarkably better than that between the CIS and experimental result. The singlet exciton binding energy obtained from the B3LYP/6-31G* calculation is 0.3 eV, which compares well with the experimental value (0.4 eV). It was shown that TDDFT employing such pure exchange function-

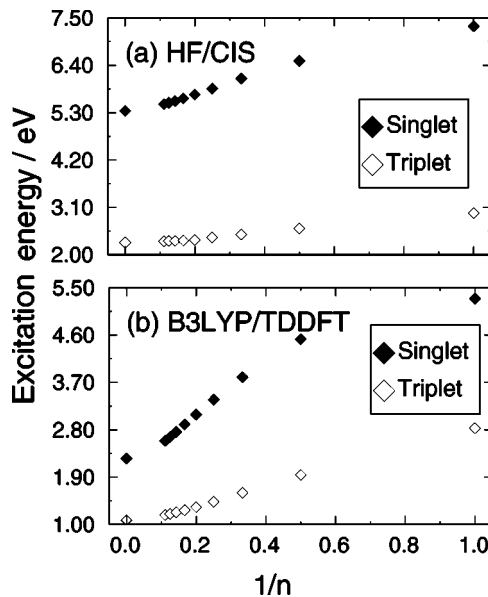


FIG. 4. The excitation energies to the lowest-lying singlet (closed diamond) and triplet (open diamond) exciton states of PDA plotted as a function of the inverse of the number of C_4H_2 units (n) calculated at the CIS/STO-3G and B3LYP/STO-3G levels. The left most plots correspond to values for the infinite polymer.

als such as Slater and Becke88 functionals is not capable of reproducing a nonvanishing exciton binding energy for some polymeric systems (e.g., polyethylene).³² This phenomenon is traced back to the incorrect asymptotic behavior or incomplete cancellation of the self-interaction energy in these pure exchange functionals. TDDFT employing hybrid functionals such as B3LYP suffers less from this problem owing to the fraction of the HF exchange in the functional, which is reminiscent of the slightly better description of Rydberg states provided by hybrid TDDFT than that by pure TDDFT.^{79,81} Indeed, mixing of the HF exchange and pure exchange functional seems responsible for the cancellation of errors in the excitation energies between CIS and pure TDDFT, which may result in the much better agreement between B3LYP and experiment than that between CIS and experiment for PDA. Both of our CIS and TDDFT calculations indicate that there is a triplet exciton state lying lower than the lowest singlet exciton state. The excitation energy to the triplet exciton state is about 0.7 eV according to the B3LYP/6-31G* calculation and is consistent with the MPPT(2) result (0.6–0.9 eV) with some empirical corrections of the polarization effects.⁹

Figure 4 plots the excitation energies to the lowest singlet and triplet excited (exciton) states of oligomers and of an infinitely long chain of PDA computed by the CIS and TDDFT methods as a function of the inverse of the chain length. These plots demonstrate that the excitation energies of oligomers smoothly but rather slowly converge at the limiting values obtained from the CO or periodic DFT calculations. The excitation energies exhibit an approximately linear behavior with respect to $n-1$ (n : the number of C_4H_2 units), which may be interpreted in terms of the terminal effect. Unlike the total energy, from which the terminal effect can be rather neatly eliminated by taking the energy difference

between oligomers of different chain lengths (as the total energy is an extensive property and can be added or subtracted), it is not straightforward to remove the terminal effect from the excitation energy, which is an intensive property. Thus for the excitation energy calculations, methods based on CO theory or periodic DFT will be particularly effective compared with the oligomer extrapolation technique.

IV. CONCLUSION

In this article we present a comprehensive theoretical account of one of the experimentally best-characterized polymeric systems, i.e., polydiacetylenes. Complete geometry optimizations are followed by the vibrational frequency calculations for all the $k=0$ modes at the HF and B3LYP levels for PDA. From these calculations we find that the HF and particularly the B3LYP calculations with an appropriate basis set provide satisfactory results for the geometrical parameters and vibrational frequencies of PDA, which compare well with the corresponding experimental data. We compute the relative stability of PDA and PBT and the potential energy curve along the transition between PDA and PBT at the HF, B3LYP, and MBPT(2) levels. Two minima are found only at the HF level of theory with the relative stability of 50 kJ/mol^{-1} favoring the PDA structure. No minimum is found for the PBT structure at the MBPT(2) and B3LYP level of theory.

The IP and EA of PDA are calculated at the HF, B3LYP, and MBPT(2) levels. Koopmans' approximation with the 6-31G* basis set tends to overestimate the IP and excessively underestimates the EA. Inclusion of the electron correlation by MBPT(2) improves the IP and EA obtained from the HF calculations significantly, but there still remain substantial errors between the calculated and experimental values. In contrast, the B3LYP/6-31G* provides reasonable values of IP and EA as the negatives of the HOMO and LUMO energies, respectively. The calculated IP and EA are 4.8 and 3.2 eV, respectively, which compares relatively well with the corresponding experimental values, 5.2–5.8 and 3.1–3.4 eV.

We also compute the vertical excitation energies to the lowest singlet and triplet exciton states by CIS and TDDFT with the B3LYP functional. Both the CIS and TDDFT (B3LYP) methods are capable of accounting for the binding energies of excitons, i.e., the nonvanishing energy differences between E_g and the excitation energies. The CIS/6-31G* excitation energy to the singlet exciton (3.7 eV) is noticeably higher than the experimental value (~ 2.0 eV), but the magnitude of the error is modest considering the error in the band gap between the HF/6-31G* result and experiment. The overestimation may be interpreted as the indication of the greater significance of diffuse basis functions in the accurate computation of EA than in that of excitation energies to the valence exciton states. The TDDFT method with the B3LYP functional again provides a reasonable excitation energy to the singlet exciton (1.4 eV). The calculated exciton binding energy (0.3 eV) compares well with the experimental value (0.4 eV).

We find that the DFT with B3LYP functional provides a rather well-balanced description of the geometries, vibra-

tional frequencies, energetics, IP, EA, E_g , and excitation energies. The B3LYP functional was originally designed to predict the thermochemical quantities accurately, and hence the good results obtained from the present B3LYP calculations for the energetics, geometries, and vibrational frequencies, which are associated directly with the total energies, attest to the fact that the functional is quite effective not only for small molecules but also for infinitely extended systems such as polymers. However, this hybrid functional appears to provide much better descriptions also for the IP, EA, E_g , and excitation energies than HF (CIS) or DFT using pure exchange-correlation functionals. The agreement between the B3LYP and experimental results may, in many cases, be traced back to the cancellation of errors between the HF and DFT portion of the hybrid functionals, but this cancellation seems to occur systematically across different properties. In this view, it would be interesting to design a hybrid functional on the basis of not only the thermochemical quantities, but also IP, EA, E_g , and excitation energies across different molecules and polymers.

ACKNOWLEDGMENTS

We appreciate useful discussions with Professor G. Wegner. This work was supported by National Science Foundation under Grant No. 980015.

- ¹ *Polydiacetylenes*, NATO ASI E102, edited by D. Bloor and R. R. Chance (Nijhoff, The Hague, 1985).
- ² G. Wegner, *Makromol. Chem.* **154**, 35 (1972).
- ³ D. Bloor, L. Koski, G. C. Stevens, F. H. Preston, and D. J. Ando, *J. Mater. Sci.* **10**, 1678 (1975).
- ⁴ A. J. Merveger and R. H. Baughman, *J. Polym. Sci., Part A-2* **11**, 603 (1973).
- ⁵ D. Bloor, F. H. Preston, D. J. Ando, and D. N. Batchelder, *Structural Studies of Macromolecules by Spectroscopic Methods*, edited by K. J. Ivin (Chichester, Wiley, 1976), p. 91.
- ⁶ D. Bloor, G. C. Stevens, P. J. Page, and P. M. Williams, *Chem. Phys. Lett.* **33**, 61 (1975).
- ⁷ J. Kiji, J. Kaiser, G. Wegner, and R. C. Schulz, *Polymer* **14**, 433 (1973).
- ⁸ A. Karpfen, *J. Phys. C* **13**, 5673 (1980).
- ⁹ S. Suhai, *Phys. Rev. B* **29**, 4570 (1984).
- ¹⁰ Y. Toyozawa, *Prog. Theor. Phys.* **12**, 422 (1954).
- ¹¹ A. B. Kunz, *Phys. Rev. B* **6**, 606 (1972).
- ¹² S. Suhai, *Chem. Phys. Lett.* **96**, 619 (1983); *Phys. Rev. B* **27**, 3506 (1983).
- ¹³ D. S. Boudreaux and R. R. Chance, *Chem. Phys. Lett.* **51**, 273 (1977).
- ¹⁴ J. W. Mintmire and C. T. White, *Phys. Rev. B* **35**, 4180 (1987).
- ¹⁵ P. Vogl and D. K. Campbell, *Phys. Rev. Lett.* **62**, 2012 (1989).
- ¹⁶ J. Ashkenazi, W. E. Pickett, H. Krakauer, C. S. Wang, B. M. Klein, and S. R. Chubb, *Phys. Rev. Lett.* **62**, 2016 (1989).
- ¹⁷ P. Vogl and D. K. Campbell, *Phys. Rev. B* **41**, 12797 (1990).
- ¹⁸ J. Paloheimo and J. von Boehm, *Phys. Rev. B* **46**, 4304 (1992).
- ¹⁹ S. Suhai, *Phys. Rev. B* **51**, 16553 (1995).
- ²⁰ G. Del. Re, J. Ladik, and G. Biczó, *Phys. Rev.* **155**, 997 (1967).
- ²¹ J. M. André, *J. Chem. Phys.* **50**, 1536 (1969).
- ²² M. Kertész, *Adv. Quantum Chem.* **15**, 161 (1982).
- ²³ J. Ladik, *Quantum Theory of Polymers as Solids* (Plenum, New York, 1988).
- ²⁴ J. Delhalle, L. Piel, J.-L. Brédas, and J.-M. André, *Phys. Rev. B* **22**, 6254 (1980).
- ²⁵ J. M. André, D. P. Vercauteren, V. P. Bodart, and J. G. Fripiat, *J. Comput. Chem.* **5**, 535 (1984).
- ²⁶ L. Piel and J. Delhalle, *Int. J. Quantum Chem.* **13**, 605 (1978).
- ²⁷ H. Teramae, T. Yamabe, and A. Imamura, *J. Chem. Phys.* **81**, 3564 (1984).
- ²⁸ S. Hirata and S. Iwata, *J. Chem. Phys.* **107**, 10075 (1997).
- ²⁹ J.-Q. Sun and R. J. Bartlett, *J. Chem. Phys.* **104**, 8553 (1996).
- ³⁰ J.-Q. Sun and R. J. Bartlett, *J. Chem. Phys.* **107**, 5058 (1997).

- ³¹M. Vračko, B. Champagne, D. H. Mosley, and J.-M. André, *J. Chem. Phys.* **102**, 6831 (1995).
- ³²S. Hirata, M. Head-Gordon, and R. J. Bartlett, *J. Chem. Phys.* **111**, 10774 (1999), and references therein.
- ³³S. Hirata and R. J. Bartlett, *J. Chem. Phys.* **112**, 7339 (2000).
- ³⁴J. Ladik, in *Electronic Structure of Polymers and Molecular Crystals*, edited by J. M. André and J. Ladik (Plenum, New York, 1975).
- ³⁵J. W. Mintmire and C. T. White, *Phys. Rev. Lett.* **50**, 101 (1983).
- ³⁶S. Suhai, *Int. J. Quantum Chem.* **42**, 193 (1992).
- ³⁷J. M. André, D. H. Mosley, B. Champagne, J. Delhalle, J. G. Fripiat, J. L. Brédas, D. J. Vanderveken, and D. P. Vercauteren, in *METECC-94, Methods and Techniques in Computational Chemistry*, edited by E. Clementi (STEF, Caligari, 1993), Vol. B, Chap. 10, p. 423.
- ³⁸I. J. Palmer and J. Ladik, *J. Comput. Chem.* **15**, 814 (1994).
- ³⁹R. Dovesi, V. R. Saunders, C. Roetti, M. Causà, N. M. Harrison, R. Orlando, and E. Aprà, *CRYSTAL95*, University of Torino, Torino, 1996.
- ⁴⁰W. Förner, R. Knab, J. Cížek, and J. Ladik, *J. Chem. Phys.* **106**, 10248 (1997).
- ⁴¹S. Hirata, M. Tasumi, H. Torii, S. Iwata, M. Head-Gordon, and R. J. Bartlett, *POLYMER* version 1.0, 1999.
- ⁴²A. D. Becke, *J. Chem. Phys.* **98**, 5648 (1993); A. D. Becke, *Phys. Rev. A* **38**, 3098 (1988); C. Lee, W. Yang, and R. G. Parr, *Phys. Rev. B* **37**, 785 (1988).
- ⁴³W. J. Hehre, R. F. Stewart, and J. A. Pople, *J. Chem. Phys.* **51**, 2657 (1969).
- ⁴⁴W. J. Hehre, R. Ditchfield, and J. A. Pople, *J. Chem. Phys.* **56**, 2257 (1972).
- ⁴⁵P. C. Hariharan and J. A. Pople, *Theor. Chim. Acta* **28**, 213 (1973).
- ⁴⁶J. S. Binkley, J. A. Pople, and W. J. Hehre, *J. Am. Chem. Soc.* **102**, 939 (1980).
- ⁴⁷P. Császár and P. Pulay, *J. Mol. Struct.* **114**, 31 (1984).
- ⁴⁸D. I. Bower and W. F. Maddams, *The Vibrational Spectroscopy of Polymers* (Cambridge University Press, Cambridge, 1989).
- ⁴⁹M. Levy, J. P. Perdew, and V. Sahni, *Phys. Rev. A* **30**, 2745 (1984).
- ⁵⁰C. O. Almbladh and U. von Barth, *Phys. Rev. B* **31**, 3231 (1985).
- ⁵¹E. R. Davidson, *J. Comput. Chem.* **17**, 87 (1975).
- ⁵²J. Olsen, H. J. Aa. Jensen, and P. Jørgensen, *J. Comput. Phys.* **74**, 265 (1988).
- ⁵³J. B. Foresman, M. Head-Gordon, J. A. Pople, and M. J. Frisch, *J. Phys. Chem.* **96**, 135 (1992).
- ⁵⁴H. Weiss, R. Ahlrichs, and M. Häser, *J. Chem. Phys.* **99**, 1262 (1993).
- ⁵⁵R. Bauernschmitt, M. Häser, O. Treutler, and R. Ahlrichs, *Chem. Phys. Lett.* **264**, 573 (1997).
- ⁵⁶H. Teramae, *Theor. Chim. Acta* **94**, 311 (1996).
- ⁵⁷The ACES II program is a product of the Quantum Theory Project, University of Florida, J. F. Stanton, J. Gauss, J. D. Watts, M. Nooijen, N. Oliphant, S. A. Perera, P. G. Szalay, W. J. Lauderdale, S. R. Gwaltney, S. N. Beck, A. Balková, D. E. Bernholdt, K.-K. Baeck, H. Sekino, P. Rozyczko, C. Huber, J. Pittner, and R. J. Bartlett. Integral packages included are VMOL (J. Almlöf and P. Taylor); VPROPS (P. R. Taylor); and a modified version of ABACUS integral derivative package (T. U. Helgaker, H. J. Aa. Jensen, J. Olsen, P. Jørgensen, and P. R. Taylor).
- ⁵⁸C. A. White, J. Kong, D. R. Maurice *et al.*, Q-CHEM, Version 1.2, Q-Chem Inc., Pittsburgh, PA, 1998.
- ⁵⁹E. Hädicke, E. C. Mez, C. H. Krauch, G. Wegner, and J. Kaiser, *Angew. Chem.* **83**, 253 (1971).
- ⁶⁰Von D. Kobelt and E. F. Paulus, *Acta Crystallogr., Sect. B: Struct. Crystallogr. Cryst. Chem.* **B30**, 232 (1974).
- ⁶¹V. Enkelmann, *Acta Crystallogr., Sect. B: Struct. Crystallogr. Cryst. Chem.* **B33**, 2842 (1977).
- ⁶²P. A. Apgar and K. C. Yee, *Acta Crystallogr., Sect. B: Struct. Crystallogr. Cryst. Chem.* **B34**, 957 (1978).
- ⁶³D. Day and J. B. Lando, *J. Polym. Sci., Part A-2* **16**, 1009 (1978).
- ⁶⁴E. A. Perpète, B. Champagne, and B. Kirtman, *J. Chem. Phys.* **107**, 2463 (1997).
- ⁶⁵M.-H. Whangbo, R. Hoffmann, and R. B. Woodward, *Proc. R. Soc. London, Ser. A* **366**, 23 (1979).
- ⁶⁶Z. Iqbal, R. R. Chance, and R. H. Baughman, *J. Chem. Phys.* **66**, 5520 (1977).
- ⁶⁷S. Hirata, H. Torii, and M. Tasumi, *Phys. Rev. B* **57**, 11994 (1998).
- ⁶⁸A. C. Cottle, W. F. Lewis, and D. N. Batchelder, *J. Phys. C* **11**, 605 (1978).
- ⁶⁹M. W. Wong, *Chem. Phys. Lett.* **256**, 391 (1996).
- ⁷⁰A. P. Scott and L. Radom, *J. Phys. Chem.* **100**, 16502 (1996).
- ⁷¹S. Hirata, H. Yoshida, H. Torii, and M. Tasumi, *J. Chem. Phys.* **103**, 8955 (1995).
- ⁷²C. Castiglioni, J. T. Lopez Navarrete, G. Zerbi, and M. Gussoni, *Solid State Commun.* **65**, 625 (1988); G. Zerbi, C. Castiglioni, J. T. Lopez Navarrete, T. Bogang, and M. Gussoni, *Synth. Met.* **28**, D359 (1989).
- ⁷³P. Pulay, G. Fogarasi, and J. E. Boggs, *J. Chem. Phys.* **74**, 3999 (1981).
- ⁷⁴W. Spanring and H. Bässler, *Chem. Phys. Lett.* **84**, 54 (1981).
- ⁷⁵S. Arnold, *J. Chem. Phys.* **76**, 3842 (1982).
- ⁷⁶A. A. Murashov, E. A. Silinsh, and H. Bässler, *Chem. Phys. Lett.* **93**, 148 (1982).
- ⁷⁷J.-W. van der Horst, P. A. Bobbert, M. A. J. Michels, G. Brocks, and P. J. Kelly, *Phys. Rev. Lett.* **83**, 4413 (1999).
- ⁷⁸J.-W. van der Horst, P. A. Bobbert, P. H. L. de Jong, M. A. J. Michels, G. Brocks, and P. J. Kelly, *Phys. Rev. B* **61**, 15817 (2000).
- ⁷⁹R. Bauernschmitt and R. Ahlrichs, *Chem. Phys. Lett.* **256**, 454 (1996).
- ⁸⁰M. E. Casida, C. Jamorski, K. C. Casida, and D. R. Salahub, *J. Chem. Phys.* **108**, 4439 (1998).
- ⁸¹D. J. Tozer and N. C. Handy, *J. Chem. Phys.* **109**, 10180 (1998).
- ⁸²S. Ivanov, S. Hirata, and R. J. Bartlett, *Phys. Rev. Lett.* **83**, 5455 (1999).
- ⁸³J. P. Perdew, R. G. Parr, M. Levy, and J. L. Balduz, Jr., *Phys. Rev. Lett.* **49**, 1691 (1982).
- ⁸⁴J. P. Perdew and M. Levy, *Phys. Rev. Lett.* **51**, 1884 (1983).
- ⁸⁵L. J. Sham and M. Schlüter, *Phys. Rev. Lett.* **51**, 1888 (1983).
- ⁸⁶B. Reimer, H. Baessler, J. Hesse, and G. Weiser, *Phys. Status Solidi B* **73**, 709 (1976).
- ⁸⁷P. Piaggio, R. Tubino, A. Borghesi, C. Dell'Erba, G. Garbarino, and L. Moramarco, *Phys. Rev. B* **45**, 6802 (1992).